A Durable Alternative for Proton-Exchange Membranes: Sulfonated Poly(Benzoxazole Thioether Sulfone)s

*Dan Zhao, Jinhuan Li, Min-Kyu Song, Baolian Yi, Huamin Zhang, and Meilin Liu**

To develop a durable proton-exchange membrane (PEM) for fuel-cell applications, a series of sulfonated poly(benzoxazole thioether sulfone)s (SPTESBOs) are designed and synthesized, with anticipated good dimensional stability (via acid–base cross linking), improved oxidative stability against free radicals (via incorporation of thioether groups), and enhanced inherent stability (via elimination of unstable end groups) of the backbone. The structures and the degree of sulfonation of the copolymers are characterized using Fourier-transform infrared spectroscopy, and nuclear magnetic resonance spectroscopy (^{1}H NMR and ^{19}F NMR). The electrochemical stabilities of the monomers are examined using cyclic voltammetry in a typical three-electrode cell configuration. The physicochemical properties of the membranes vital to fuel-cell performance are also carefully evaluated under conditions relevant to fuel-cell operation, including chemical and thermal stability, proton conductivity, solubility in different solvents, water uptake, and swelling ratio. The new membranes exhibit low dimensional change at 25 °C to 90 °C and excellent thermal stability up to 250 °C. Upon elimination of unstable end groups, the co-polymers display enhanced chemical resistance and oxidative stability in Fenton's test. Further, the SPTESBO-HFB-60 (HFB-60=hexafluorobenzene, 60 mol% sulfone) membrane displays comparable fuel-cell performance to that of an NRE 212 membrane at 80 °C under fully humidified condition, suggesting that the new membranes have the potential to be more durable but less expensive for fuel-cell applications.

1. Introduction

Proton-exchange membrane (PEM) fuel cells are efficient devices for direct conversion of chemical fuels to electricity and hold promise for low or zero-emission electric or hybrid electric vehicles, smart grids, and portable electronics. However, the commercialization of these fuel cells hinges on their durability and cost. Accordingly, significant efforts have shifted from improving short-term performance to enhancing long-term fuel-cell durability and reducing the cost.[1,2] To date, PEMs with a wide variety of chemical compositions and structures have been explored to find a less expensive alternative to the currently used perfluorinated sulfonic acid (PFSA) membranes but with superior properties, including high proton conductivity, good mechanical properties, excellent chemical and electrochemical stabilities, low reactant crossover, and so forth.[3]

In the past few decades, extensive efforts have been devoted to unraveling the mechanism of membrane degradation[4–8] to effectively improve their stabilities under fuel-cell operating conditions.[9–19] Several effective strategies have been developed, including polytetrafluoroethylene (PTFE) or polyvinylidene fluoride (PVdF) reinforcement to enhance mechanical strength[16–19] and dispersion of free-radical scavengers[10,11] or H_2O_2 decomposition catalysts[14,15] to suppress the formation of oxidative species (HO•/HO_2•, and H_2O_2). However, some weak points and unstable end groups in the polymer structures are still susceptible to attacks that may lead to membrane degradation.[20,21] The best strategy to mitigate these potential degradation problems is to introduce antioxidative groups to shield weak points and to eliminate unstable end groups from the polymer structures.

Among the sulfonated hydrocarbon membranes widely studied,[22] the sulfonated poly(arylene thioether)s are considered most promising[23–30] because of their good film-forming capabilities, hydrophilicity, high proton conductivity,[23] and oxidative stability.[27,28] In particular, the oxidative species (H_2O_2,

D. Zhao, Dr. J. H. Li, M.-K. Song, Prof. M. L. Liu
Center for Innovative Fuel Cell and Battery Technologies
School of Materials Science and Engineering
Georgia Institute of Technology
Atlanta, GA 30332–0245, USA
E-mail: meilin.liu@mse.gatech.edu
D. Zhao, Prof. B. L. Yi, Prof. H. M. Zhang
Lab of PEMFC Key Materials and Technologies
Dalian Institute of Chemical Physics
Chinese Academy of Sciences
457 Zhongshan Road, Liaoning, Dalian 116023, P.R. China
D. Zhao
Graduate School of the Chinese Academy of Sciences
Beijing 100039, P.R. China
Dr. J. H. Li
College of Materials Science and Technology
Nanjing University of Aeronautics and Astronautics
Nanjing 210016, P.R. China

DOI: 10.1002/aenm.201000062

HO•, and HO_2•)generated under fuel-cell operating conditions could be consumed inside the polymer networks by the conversion of the electron-donating thioether group (–S–) into an electron-withdrawing group (sulfone group $–SO_2–$ and/or sulfoxide group –SO–),[30] so that it can function as a free-radical-scavenging moiety. Like most sulfonated aromatic polymers, however, the simple sulfonated poly(arylene thioether)s require a high degree of sulfonation to achieve sufficient proton conductivity, due mainly to the low acidity of the sulfonic groups in the aromatic rings. Such a high sulfonation level often leads to dramatic swelling in hydrated states, and even solubility in methanol–water solution.[31]

Acid–base cross-linking is an effective method to improve dimensional stability and avoid irreversible swelling.[32–34] Introduction of nitrogen-containing heterocyclic rings into the sulfonic polymer backbone is a facile way to achieve this crosslinking. Among heterocyclic polymers, polybenzoxazoles (PBOs) exhibit excellent thermal and oxidative stability, high tensile strength, and good solvent and acid resistance.[35] Liet al.[36] successfully synthesized soluble sulfonated PBO polymers and reported high proton conductivities over a wide range of temperatures and humidities.

In our effort to develop durable and inexpensive PEMs, we have designed and synthesized sulfonated poly(benzoxazole thioether sulfone)s (SPTESBO) using an aromatic substitution polycondensation. The anticipated unique advantages of these materials are as follows: The basic benzoxazole structure will offer dimensional stability of the sulfonated backbone through acid–base crosslinking, whereas the thioether groups in the backbone will improve the oxidative stability of the polymer by resisting free-radical attack. Further, the introduction of hexafluorobenzene (HFB) as the end-capping and coupling agent is expected to eliminate unstable end groups, thus further enhancing the chemical oxidative stability of the copolymers. In this study, we have systematically evaluated the inherent properties of these polymer structures vital to membrane durability (such as thermal, chemical, oxidative, and electrochemical stability) as well as other physicochemical properties important to fuel-cell performance, including proton conductivity, solubility, water uptake, and swelling ratio. In addition, PEMs based on these copolymers were tested in fuel cells to characterize the properties and performances under practical fuel-cell operating conditions.

2. Results and Discussion

2.1 Synthesis and Characterization

SPTESBO-*X* with various degrees of sulfonation ["*X*" represents the molar percentage of disodium 3,3'-disulfonated-4,4'-difluorodiphenyl sulfone (SDCDPS) in the copolymers] were synthesized by random copolymerization of 2,2'-bis[2-(4-fluorophenyl) benzoxazol-6-yl] hexafluoropropane (6FBO), SDCDPS, and 4,4'-thiobisbenzenethiol (TBBT) in *N,N*-dimethylacetamide (DMAc) in the presence of milled anhydrous potassium carbonate at 160 °C for 20 h (as shown in **Figure 1**). The molar ratio of 6FBO to SDCDPS was controlled at 100:0, 80:20, 60:40, and 40:60 to obtain copolymers with different ion-exchange capacities (IECs; shown in **Table 1**).

Figure 2 shows some typical ^{1}H NMR spectra of SPTESBO-*X* with peak assignments. Integration of the ^{1}H NMR signals was used to calculate the sulfonation degree (SD), which represents the actual mole percentage of sulfonated unit per average repeat unit in the obtained copolymers. The ratio of the integration value of H7 to H1 was used for the calculation (shown in Table 1). The results indicate that the copolymerization was successfully achieved.

To introduce hexafluorobenzene (HFB) with six active fluorine atoms (i.e., the end-capping and coupling agent), the reaction temperature was cooled down to 80 °C and the nitrogen purge was stopped. When HFB was added dropwise and the reaction was allowed to proceed for 12 h, the "Weissenberg effect" was observed, an indication of molecular-weight increase. To obtain polymer fibers, DMAc was added to dilute the polymer solution at 60 °C. The solution then coagulated in methanol and was filtered. **Figure 3** schematically shows the synthesis of copolymer SPTESBO-HFB-*X* with HFB linkage and end-capping.

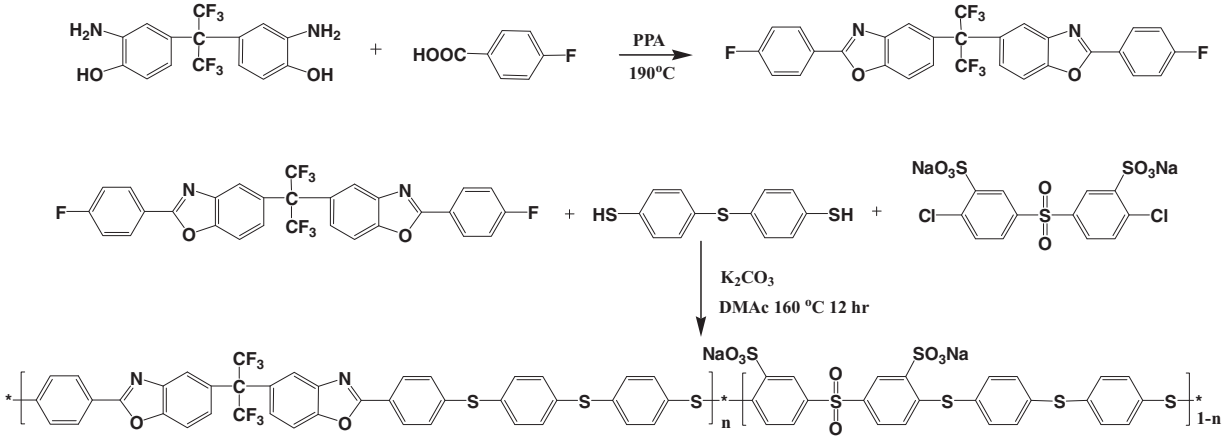

Figure 1. Synthesis of copolymers SPTESBO-*X*.

wTable 1. Results of polycondensation reactions.

Sample	Feed ratio[a)] [mol%]	SD[b)] [%]	Yield [%]	η [dL g^{-1}]	IEC [meq g^{-1}]		σ[c)] [S cm^{-1}]
					Calc.	Found	
PTEBO	100/0/100	0	97	1.19	0	-	-
SPTESBO-20	80/20/100	23.7	95	0.96	0.61	0.34	0.017
SPTESBO-40	60/40/100	43.1	93	0.86	1.16	0.83	0.052
SPTESBO-60	40/60/100	64.5	90	0.83	1.81	1.04	0.13
PTEBO-HFB	100/0/100	0	98	1.89	0	-	-
SPTESBO-HFB-20	80/20/100	25.0	97	1.46	0.65	0.41	0.024
SPTESBO-HFB-40	60/40/100	50	95	1.47	1.36	0.92	0.078
SPTESBO-HFB-60	40/60/100	56.5	96	1.67	1.56	1.10	0.13

[a)]Feed ratio of the monomer: 6FBO/SDCDPS/TBBT; [b)]SD (sulfonation degree) was calculated from the ratio of the signal integration in ^{1}H NMR measurements; [c)]The proton conductivity was measured at room temperature under fully humidified condition. The proton conductivity of NRE 212 membrane was 0.13 S cm^{-1} under the same conditions.

The ^{1}H NMR and ^{19}F NMR spectra of SPTESBO-HFB-40 are shown in **Figure 4**. No significant changes occurred in the ^{1}H NMR spectrum compared to that of SPTESBO-40. The coupling reaction was confirmed by ^{19}F NMR spectroscopy. As shown in Figure 4 B, the spectrum of the copolymer has a sharp singlet at –157.9 ppm [the fluorine atoms in –C(CF$_3$)$_2$– correspond to the peak at –58.3 ppm], which implies that the coupling reaction exclusively proceeded at the *para* position of the HFB moieties.[37] If the coupling reaction occurred at the *ortho* or *meta* position, the spectrum would show two or three peaks from the HFB moieties, respectively. The amount of HFB consumed in the end-capping reaction was too small to observe peaks arising from the end-caps in the ^{19}F NMR spectrum.

The FTIR spectra of SPTESBO-*X* and SPTESBO-HFB-*X* with various SD indicated that all polymers displayed the characteristic absorption bands at 1596 cm^{-1} (benzoxazole, –C=N stretching) and 1049 cm^{-1} (benzoxazole, C–O streching).[36] The absorption at 1086 cm^{-1} was assigned to the asymmetric vibration of the sulfonated groups, and the band at 620 cm^{-1} was attributed to the stretching vibration of the S–O of the sulfonated groups.[40]

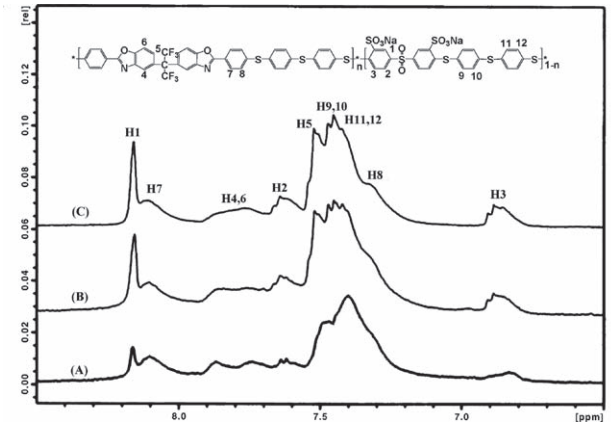

Figure 2. ^{1}H NMR spectra of copolymers SPTESBO-*X* with *X* = A) 20, B) 40, and C) 60

The results of the polycondensation reaction are summarized in Table 1. In all cases, the yields were above 90%, and the intrinsic viscosities were greater than 0.8 dL g^{-1} in *N*-methyl-2-pyrrolidone (NMP) at 25 °C. These results indicate that all the products were of high molecular weight. Moreover, the SPTESBO-HFB-*X* polymer showed higher intrinsic viscosities than SPTESBO-*X* with similar SD; this is another indication that the coupling reaction with HFB occurred during the polymerization process.

The IECs of the sulfonated polymers determined by titration increased reasonably with the increase in sulfonation degree. The actual IECs of the membranes were somewhat lower than the calculated values, which was attributed to the formation of hydrogen bridges or the protonation of the basic N atom in the oxazole ring by the H atoms from the sulfonic acid groups.[34,36,41] Nevertheless, the proton conductivities of the membranes were still reasonably high. For example, the proton conductivities of both SPTESBO-60 and SPTESBO-HFB-60 are about 0.13 S cm^{-1} at room temperature under fully humidified conditions, which is comparable to that of NRE 212 membrane under the same conditions.

2.2. Stability Studies

2.2.1. Electrochemical Stability of the Monomers

Figure 5 shows some typical cyclic voltammograms (CVs) of the monomer TBBT and the model compound. An obviously irreversible oxidation peak appeared at +1.3 V (vs. normal hydrogen electrode; NHE) for benzoxazole. However, the model compound was oxidized at even higher potential (>+1.6 V vs. NHE). The effect of chemical structure on the electrochemical stability could be rationalized by considering the electron distribution of the oxazole ring. The benzo aromatic ring and the 2-phenyl group next to the oxazole ring form a larger conjugated, planarstructure, which could decrease the negative charge on the oxazole ring and increase the molecular electrochemical stability. The TBBT molecule contains two kinds of groups; thioether bond (–S–) and thiol group (–SH), both of which can be easily oxidized. As clearly shown in Figure 5 A, an irreversible oxidation peak appeared

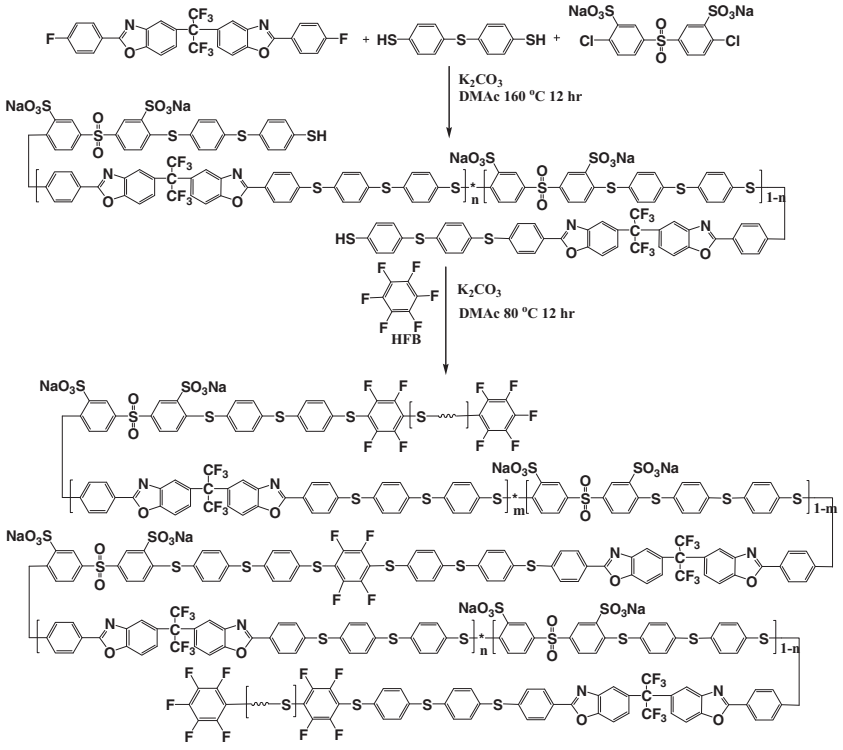

Figure 3. Synthesis of copolymers SPTESBO-HFB-*X* with coupling and end-capping.

near +1.4 V (vs. NHE) in the voltammogram for TBBT. Moreover, an even larger peak appeared at higher potential (>+1.8 V vs. NHE). The current density decreased dramatically with the number of cycles. The height of the oxidation peak, which was obvious in the very first positive scan, diminished dramatically in the second and fifth cycles. It seems that the oxidation products of TBBT were absorbed on the surface of the platinum electrode and, thus, blocked the active sites for further oxidation.

Two possible explanations of this oxidation behavior are as follows. First, the two oxidation peaks correspond to two oxidation steps of sulfur atoms; as shown in **Figure 6**A the thioether bond (–S–) was oxidized to a sulfoxide group (–SO–), and then to a sulfone group ($–SO_2–$). Second, the two oxidation peaks are attributed to the oxidation of the thioether bond (–S–) and thiol group (–SH), respectively, as schematically shown in Figure 6B. For the electrochemical oxidation in dimethyl formamide (DMF) without water, the thiol groups mainly followed the thiol/disulfide cross-linked reaction.[42]

To clarify the oxidation process, three model molecules, phenyl sulfide, phenyl sulfoxide, and phenyl sulfone, were studied using the same procedures. No obvious redox peaks were observed for phenyl sulfoxide and phenyl sulfone in a wide potential range (0 to +1.8 V vs. NHE). In contrast, the oxidation peak of phenyl sulfide is similar to that of the second peak of TBBT, which implies that the oxidation peak at +1.4 V (vs. NHE) is not due to the oxidation of the thioether bond (–S–), but to the oxidation of the thiol group (–SH). Thus, the oxidation of TBBT is most likely described by the schematic shown in Figure 6B. The CVs for TBBT indicate that the thiol group is unstable under fuel-cell operating conditions. These unstable end groups are believed to be the origin of chemical/electrochemical oxidation degradation of PEM.[20,21] Therefore, the elimination of these unstable end groups is a necessary step in achieving durable polymer materials for PEM fuel cells.[43]

2.2.2. Oxidative Stability

The oxidative stability of SPTESBO-*X* and SPTESBO-HFB-*X* membranes was investigated in Fenton's reagent (3 wt.% H_2O_2, 2 ppm $FeSO_4$) at 80 °C to accelerate the test. The elapsed time when the membranes dissolved completely (τ)[44] and their weight losses after being maintained at 80 °C for 1 h are summarized in **Table 2**. All membranes had a τ value of ~10–30 h, higher than other oxidation-proof aromatic membranes under the same conditions.[46] However, it was observed that a higher IEC led to lower oxidative stability. The SPTESBO-60 dissolved completely in about 10 h. Compared to the SPTESBO-X copolymers, the oxidative stability of SPTESBO-HFB-*X* membranes improved considerably because of the elimination of the unstable end groups.

All the polymers showed a weight increase after treatment with Fenton's reagent at 80 °C for 1 h. The weight gain was possibly associated with the oxidation of sulfide (–S–) via sulfoxide (–SO–) to sulfone ($–SO_2–$) units as recorded by Schuster et al.[30] **Figure 7** confirms the oxidation process. After the Fenton's reagent treatment, the asymmetric and symmetric stretch of sulfoxide groups were observed apparently at ~1030–1040 cm^{-1} and ~1090–1100 cm^{-1} and their intensity increased with soaking time.[28,30,46] The transformation of sulfide groups into sulfoxide groups by reaction with HO• or HO_2• radicals avoided the direct attack of the polymer backbones by the oxidative species. Thus, SPTESBO-HFB-*X* membranes are expected to exhibit superior durability in fuel-cell applications.

2.2.3. Thermal Properties

The thermal stability of SPTESBO-*X* and SPTESBO-HFB-*X* copolymers in the acid form was evaluated using TGA in N_2. The TGA traces of the resulting products are presented in **Figure 8**. The onset $–SO_3H$ splitting off temperatures (T_{-SO3H}) are listed in Table 2. The TGA curves suggest two distinct weight-loss processes. The first process at ~250 °C (T_{-SO3H}) is attributed to the loss of sulfonic groups, while the second at ~500 °C is related to fragmentation of the main chain.[36,41] The results clearly indicate that the copolymers are thermally stable within the temperature range for PEMFC applications. However, it appears that the coupling and end-capping reactions had no observable effect on the thermal stability of the $–SO_3H$ group and the main chain.

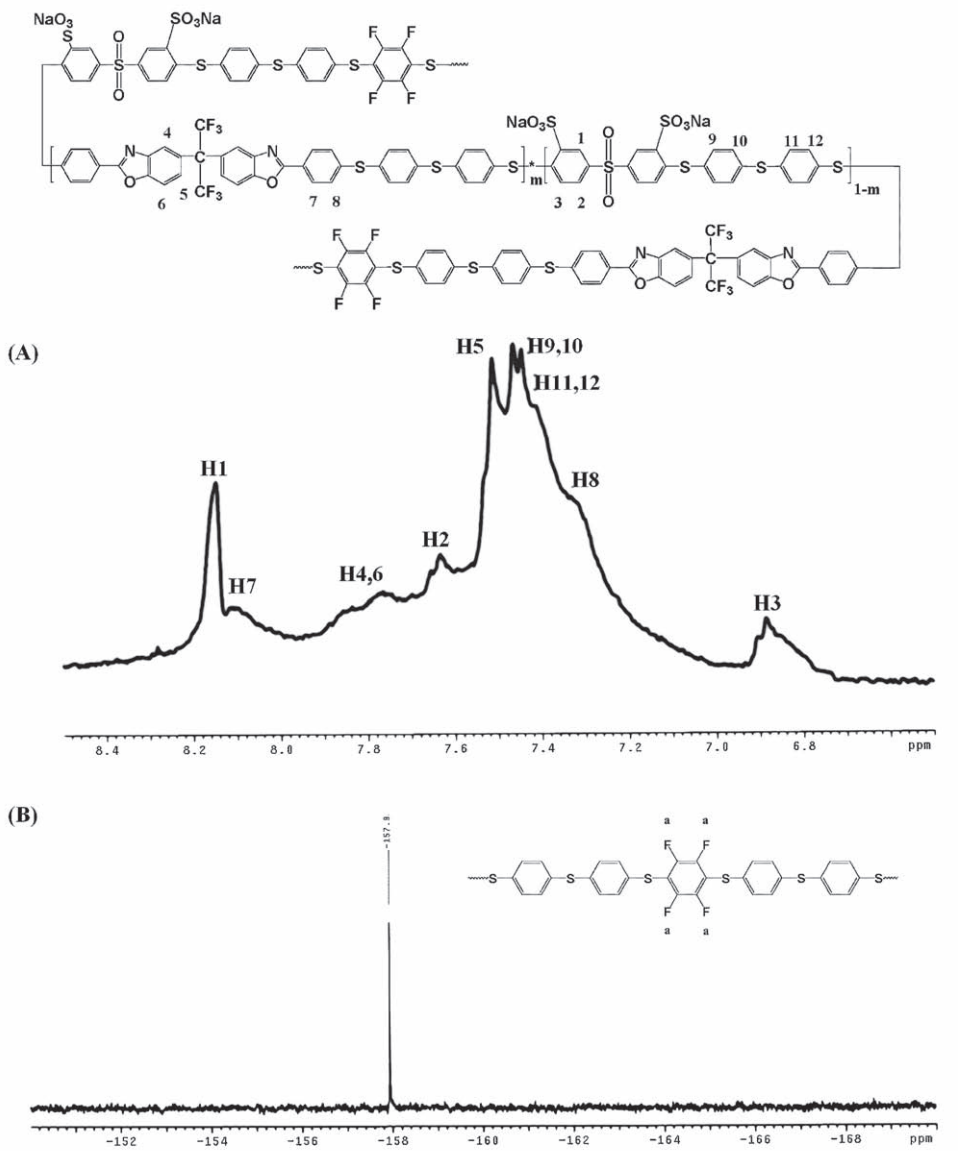

Figure 4. A) ^{1}H NMR and B) ^{19}F NMR spectra of copolymer SPTESBO-HFB-40.

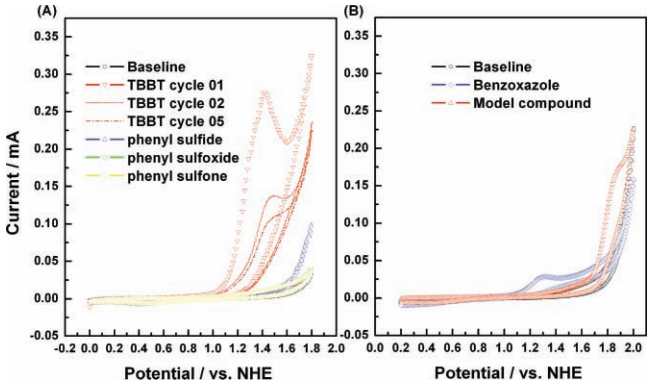

Figure 5. Typical CVs of monomers TBBT and model compound with a concentration of ~5 × 10^{-3} mol·dm^{-3} in 0.1 mol·dm^{-3} TBAPF6-CH_3CN solution at 25 °C. The potential sweep rate was kept at 10 mV s^{-1}.

2.3. Solubility

The solubility data for SPTESBO-*X* and SPTESBO-HFB-X in different solvents (at a polymer loading of 0.05g mL^{-1}) are summarized in **Table 3**. No polymer samples displayed observable solubility in chloroform, methanol, or water. The polymers were soluble in NMP and can be readily cast into homogeneous membranes for further evaluation and testing.

2.4. Water Uptake and Swelling Ratios

The water uptake and swelling ratios of PEMs greatly influence proton conductivity, dimensional stability, and mechanical strength. To obtain a good balance between the proton conductivity and mechanical integrity, the water uptake should be

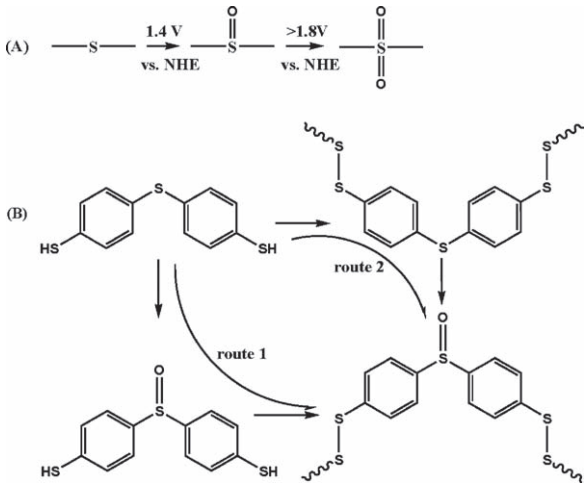

Figure 6. Proposed oxidation processes for monomer TBBT.

Table 2. Thermogravimetric analysis (TGA) and oxidative stability results of SPTESBO-*X* and SPTESBO-HFB-*X*.

Membrane	Thickness [μm]	Residue[a)] [%]	$\tau^{b)}$[h]	T_{-SO3H} [°C]
PTESBO	60	103.1	>200	-
SPTESBO-20	58	102.7	21.5	261
SPTESBO-40	60	103.4	18.6	253
SPTESBO-60	61	102.8	10.0	247
PTESBO-HFB	57	103.5	>200	-
SPTESBO-HFB-20	60	103.9	30	263
SPTESBO-HFB-40	59	103.8	25	257
SPTESBO-HFB-60	60	103.1	18	248

[a)]Residual weight of membranes after treatment in Fenton's reagent for 1 h at 80 °C; [b)] refers to the time when the membrane dissolved completely.

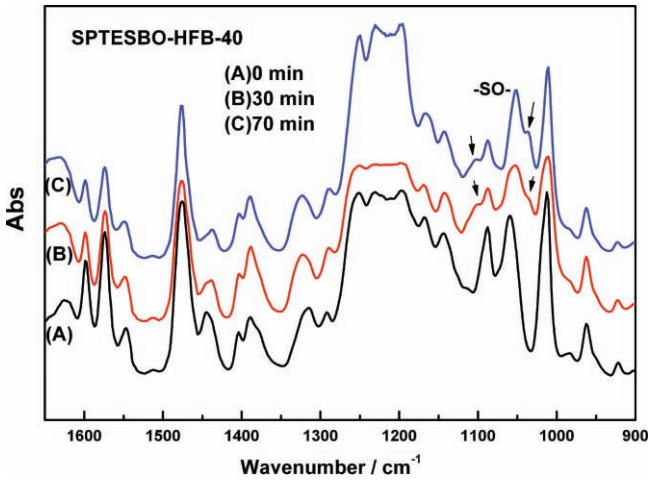

Figure 7. FTIR spectra of SPTESBO-HFB-40 membrane after being soaked in Fenton's reagent for different periods of time.

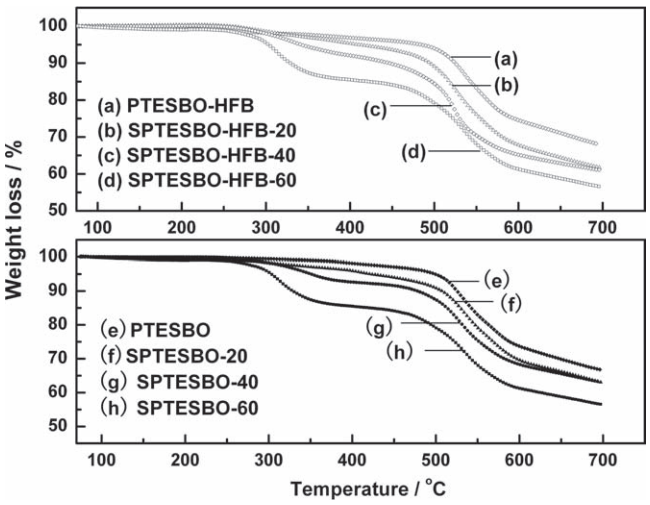

Figure 8. TGA curves of SPTESBO-*X* and SPTESBO-HFB-*X* membranes in acid form acquired in nitrogen with a temperature sweep rate of 10 °C min^{-1}.

controlled within a reasonable range.[45] As shown in **Figure 9**, the water uptake and swelling ratios increase gradually with increasing temperature and sulfonation degree. Moreover, SPTESBO-60 and SPTESBO-HFB-60, with the highest sulfonation degree, displayed relatively low water uptake (~35%–40%) and swelling ratios (~14%–17%) at 90 °C, which suggests that they could be operated at elevated temperature with excellent dimensional stability. The improvement of the dimensional stability could be attributed to the acid–base crosslinking between the nitrogen atoms of the benzoxazole moieties and the sulfonic acid groups inside the polymer networks. It is worth noting that the SPTESBO-HFB-*X* membrane displayed lower water uptake and swelling than those of SPTESBO-X with a similar SD. This result is attributed to the introduction of HFB into the polymer backbone, which improves the hydrophobic property of the membranes.

2.5. Fuel-Cell Performance

The electrochemical behavior of the SPTESBO-HFB-*X* membranes (~55 μm) was further evaluated in a fuel cell at 80 °C under fully humidified conditions. The performances of SPTESOB-HFB-60 and SPTESBO-HFB-40 membranes are compared directly with that of a commercially available NRE 212 membrane in **Figure 10**A. The cell performance improved with increasing disulfonated monomer, due to enhanced proton conductivity. As the content of disulfonated monomer increased from 40% to 60%, the cell voltage increased from ~0.42 to ~0.56 V at a constant current density of 1000 mA cm^{-2}, which corresponds to a peak power-density increase from ~420 to ~640 mW cm^{-2}. The SPTESBO-HFB-60 membrane exhibited comparable cell performance to that of the NRE 212 membrane under the test conditions, consistent with the proton conductivity data. Thus, our membranes have good potential to be a cost-effective and durable alternative PEM for fuel-cell applications. It is noted, however, that the performances of SPTESBO-HFB-60 membranes decreased as the

Table 3. Solubility of SPTESBO-*X* and SPTESBO-HFB-*X*.

	Solvents[a]						
Polymer	NMP	DMSO	DMF	DMAc	$CHCl_3$	Methanol	H_2O
PTESBO	+	–	–	+–	–	–	–
SPTESBO-20	+	+	+	+	–	–	–
SPTESBO-40	+	+	+	+	–	–	–
SPTESBO-60	+	+	+	+	–	–	–
PTESBO-HFB	+	–	–	–	–	–	–
SPTESBO-HFB-20	+	+–	+–	+	–	–	–
SPTESBO-HFB-40	+	+	+	+	–	–	–
SPTESBO-HFB-60	+	+	+	+	–	–	–

[a]The test was performed at a sample loading of 0.05g mL^{-1}. (+) soluble; (–) insoluble in the temperature range from 25 °C to the boiling point of the solvent; (+–) partially soluble or swelling on heating.

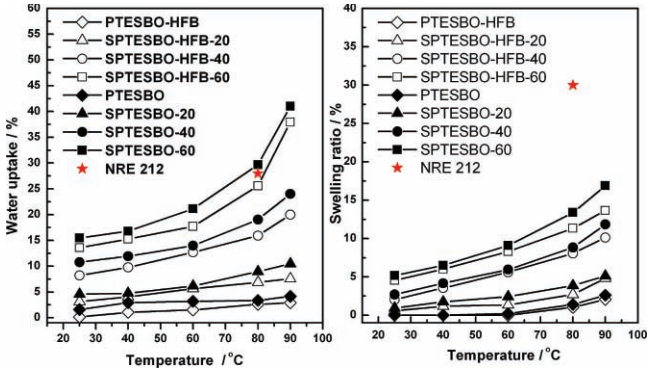

Figure 9. Water uptake and swelling ratios of SPTESBO-*X* and SPTESBO-HFB-*X* measured at different temperatures.

relative humidity was reduced, as seen in Figure 10B. To reduce the dependence on relative humidity at elevated temperatures, free-radical-scavenging catalysts[11,15] and water-retention particles[47] should be incorporated into the composite membranes; this provides direction for further enhancement of other performance characteristics.

3. Conclusions

The SPTESBO-*X* copolymers were successfully synthesized. HFB was introduced as the end-capping and coupling agent to eliminate unstable end groups in the SPTESBO-*X* copolymers and to increase their molecular weight. The structures and sulfonation degree of the copolymers were verified by FTIR and ^{1}H NMR and the existence of the HFB linkage groups was confirmed by ^{19}F NMR. Cyclic voltammograms suggest that TBBT displays two large irreversible oxidation peaks due to the presence of the unstable group (–SH), which indicates the necessity to eliminate unstable end groups. All copolymers were successfully cast into homogeneous membranes using NMP as a solvent. The copolymers also displayed excellent dimensional stability because of the formation of an acid–base complex between the N atoms of the benzoxazole moieties and the $-SO_3H$ groups. All copolymers showed good thermal stability up to 250 °C and excellent oxidative stability. The improved oxidation resistance of these polymers can be attributed to the oxidation of sulfide groups (–S–) to sulfoxide groups (–SO–) in the presence of free radicals and the elimination of unstable end groups. Further, the SPTESBO-60 and SPTESBO-HFB-60 copolymers exhibited comparable proton conductivities to that of NRE 212 at room temperature under fully humidified conditions. In particular, fuel cells based on a SPTESBO-HFB-60 membrane demonstrated comparable performance to that of a commercial NRE 212 membrane, which implies that, indeed, sulfonated poly(benzoxazole thioether sulfone)s have great potential to be cost-effective and durable membranes for fuel-cell applications.

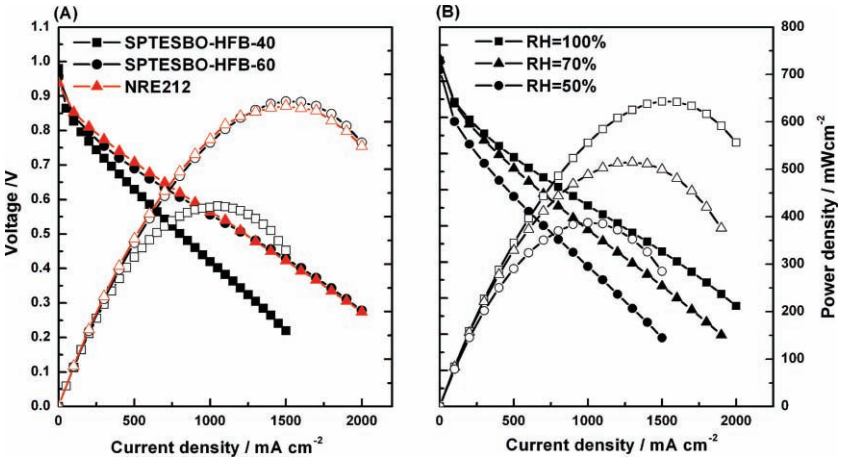

Figure 10. A) Typical performances of fuel cells based on SPTESBO-HFB-40, SPTESBO-HFB-60, and NRE 212 membranes at 80 °C under 0.2 MPa H_2 and O_2 with 100% relative humidity; B) typical performance of a fuel cell based on a SPTESBO-HFB-60 membrane at 80 °C with different relative humidities: 100%, 70%, and 50%.

4. Experimental Section

Materials: Chemicals were received from Fisher Chemical Co., Sigma-Aldrich Co., Alfa-Aesar Co., and TCI America Chemical in p.a. quality and used without further purification. Toluene (Fisher Chemical Co.) was dried over molecular sieves (3A beads, 4–8 mesh, Aldrich Chemical Co.) and filtered before use. 4,4'-Thiobisbenzenethiol (98%, Sigma-Aldrich Co.) was recrystallized from toluene and dried at 80 °C overnight. The 2,2'-bis [2-(4-fluorophenyl)benzoxazol-6-yl]hexafluoropropane (6FBO) and disodium 3,3'-disulfonated-4,4'-difluorodiphenyl sulfone (SDCDPS) were synthesized according to procedures described elsewhere.[25,36]

Synthesis of Model Compound (2,2'-Diphenyl-5,5'-Bibenzoxazole): Benzoic acid (1.23 g, 10 mmol) and 2,2-bis(3-amino-4-hydroxyphenyl) hexafluoropropane (BAHBP) (1.10 g, 5 mmol) were dissolved in 15 g polyphosphoric acid (PPA) in a 100-mL three-necked flask equipped with magnetic stirrer, nitrogen inlet/outlet, and condenser. The same process was followed as for the synthesis of monomer 6FBO. Yield: 70%. 1H NMR (400 MHz, $CDCl_3$, δ): 8.32~8.28 (m, 4H), 7.87 (s, 2H), 7.85 (d,2H, |J|=12 Hz), 7.67~7.65 (q, 2H), 7.58~7.56 (m, 4H), 7.56~7.54 (m, 2H), as shown in Figure S1 of the Supporting Information.

Synthesis of the Sulfonated Poly(Benzoxazole Thioether Sulfone)s: All polymers were synthesized by polycondensation via typical high-temperature nucleophilic aromatic-substitution reaction. Synthesis of the copolymer with 40% disulfonation (SPTESBO-40) is given as a representative example. In a three-necked flask equipped with a Dean–Stark trap, condenser, and nitrogen inlet, 6FBO (0.689 g, 1.2 mmol), SDCDPS (0.393 g, 0.8 mmol), TBBT (0.510 g, 2 mmol), and potassium carbonate (0.332 g, 2.4 mmol) were dissolved in a mixture of 10 mL DMAc and 10 mL toluene. The mixture was heated to 140 °C and kept there for ~4–6 h to remove the water from the system by azeotropic distillation of toluene under nitrogen. The reaction temperature was then slowly increased to 160 °C and kept there for about 20 h. The resulting viscous polymer solution was then poured into methanol, washed with water to remove any inorganic salts, and dried at 80 °C for 24 h in vacuum.

Elimination of End Groups: HFB was selected as the coupling and end-capping reagent.[37,46] For the synthesis of SPTESBO, when the temperature increased to 160 °C, the reaction was maintained for about 4 h. Then the temperature was dropped down to 80 °C. When HFB was used, the nitrogen purge was stopped at this point to prevent the loss of the HFB vapor because of the lower boiling point of HFB (80.6 °C). An aliquot of HFB was added and the reaction was allowed to proceed for 12 h. The resulting viscous polymer solution was then poured into methanol, washed with water to remove any inorganic salts, and dried in a vacuum oven at 80 °C for 24 h.

Preparation and Acidification of Membranes: The SPTESBO-*X* and SPTESBO-HFB-*X* polymers as sodium salts were dissolved in NMP. The solution (5 wt.%) was cast onto a glass substrate and dried at 70 °C for 40 h. Then the membrane was peeled off from the glass plate by immersion in deionized water, acidified by soaking in 0.5 M H_2SO_4 solution for 48 h, and rinsed with deionized water to remove the free acid in the membrane. The thickness of the membrane was ~55 μm.

Characterization: Fourier-transform infrared (FTIR) spectra were obtained from KBr pellets or membrane samples using a BRUKER EQUINOX 55 spectrometer. ^{1}H NMR and ^{19}F NMR spectra were collected on a Bruker DMX 400 instrument. Dimethyl sulfoxide-d_6 (DMSO-d_6) or chloroform-d ($CDCl_3$) were used as NMR solvents. Instrinsic viscosity (η_{int}) was measured at 25 °C in 0.05 g dL^{-1} NMP solutions with an Ubbelohde viscometer. The solubilities of SPTESBO-*X* and SPTESBO-HFB-*X* (at a polymer loading of 0.05g mL^{-1}) were investigated in different solvents.

Water Uptake and Swelling Ratio: Water uptake and swelling ratio of SPTESBO-*X* and STPESBO-HFB-*X* membranes were determined by measuring the weight and length variation before and after the hydration. The water uptake was calculated from $(W_{wet} - W_{dry})/ W_{dry}$, where W_{dry} and W_{wet} are the weights of dried and wet membranes. The swelling ratio was calculated from $(L_{wet} - L_{dry})/ L_{dry}$, where L_{dry} and L_{wet} are the lengths of dried and wet membranes.

Ion-Exchange Capacity of Membrane and Proton Conductivity: The IECs of the composite membranes were measured using the titration method.[36] The sample in -SO_3H form was immersed in a saturated NaCl solution for 24 h in order to release the H^+ ions. Then, the acid solution was titrated against 0.01 M NaOH solution. The IEC (meq g^{-1}) was calculated from IEC = $(V \times M)/m$, where V is the added titrant volume at the equivalent point (mL), M is the molar concentration of the titrant, and m is the dry sample weight (g).

Proton conductivities of the composite membranes were measured using impedance spectroscopy with a Solatron 1287 Electrochemical Interface and 1260 Frequency Response analyzer in the frequency range of 1 M Hz to 10 Hz and an applied ac voltage of 10 mV. As shown in Figure S2, the measurements were carried out in a test cell held at room temperature under fully humidified conditions. The proton conductivity, σ (S cm^{-1}), was calculated from $\sigma = d/(R \times S)$, where d is the distance between two electrodes (cm), S is the area of the electrode (cm^2), and R is the measured resistance of the membrane sample (Ω).

Electrochemical, Chemical, and Thermal Stabilities: The electrochemical stabilities of the model compound and monomer TBBT were investigated using cyclic voltammetry in a typical three-electrode cell configuration.[47] The electrolyte, 0.1 mol dm^{-3} tetrabutylammonium hexafluorophosphate (TBAPF6) in DMF solution, containing 5×10^{-3} mol dm^{-3} of monomer TBBT or the model compound, was purged with nitrogen before experiments. The potential was swept in the range of ~–0.197–1.6 V and ~0–1.8 V (vs. Ag/AgCl reference electrode) at a scan rate of 10 mV s^{-1} to investigate the stability of the monomers within the operating window of fuel cells.

Oxidative stability was investigated following a typical procedure. Membrane samples were soaked in Fenton's reagent (2 ppm $FeSO_4$ in 3wt.% H_2O_2) at 80 °C. The oxidative stability was evaluated by recording the residual weight of the membranes after treatment in Fenton's reagent for 1 h and the elapsed time when the membrane disappeared completely. The chemical structure changes of the sulfide moieties were recorded using FTIR.

The thermal stability of the SPTESBO-*X* and SPTESBO-HFB-*X* membranes in the acid form was investigated using a thermal analysis system (SDT Q600). Initially, the sample were heated under nitrogen to 150 °C for 10 min to remove the water absorbed in the samples, then cooled down to 50 °C and reheated to 700 °C at a rate of 10 °C min^{-1} under an N_2 atmosphere.

Preparation of Membrane Electrode Assembly and Single-Cell Test: Gas-diffusion electrodes with a three-layer structure were prepared as reported elsewhere.[28] The Pt/C catalyst loading in the anode and cathode were 0.3 mg Pt cm^{-2} and 0.6 mg Pt cm^{-2}, respectively. Nafion® loading was 0.4 mg cm^{-2} in both electrodes. The membrane electrode assembly (MEA) was fabricated by a hot-pressing process. A membrane with two gas diffusion electrodes (1 cm^2 of geometric area) was sandwiched and hot-pressed at 160 °C to form an MEA. The fuel cells were tested at 80 °C under fully humidified condition while both cell voltages and currents were monitored and recorded using a KFM 2030 impedance meter (Kikusui, Japan). The flow rates of inlet gases for both H_2 and O_2 were controlled at 40 mL min^{-1} at a pressure of 0.2 MPa.

Supporting Information

Supporting Information is available from the Wiley Online Library or from the author.

Acknowledgements

This material is based upon work supported as part of the Heterogeneous Functional Materials (HetroFoaM) Center, an Energy Frontier Research Center funded by the U.S. Department of Energy (DOE), Office of Science,

Office of Basic Energy Sciences under Award Number DE-SC0001061, and the WCU Program at UNIST from the Korean Ministry of Education, Science, and Technology.

Received: November 12, 2010
Revised: January 8, 2011
Published online: February 24, 2011

[1] R. Borup, J. Meyers, B. Pivovar, Y. S. Kim, R. Mukundan, N. Garland, D. Myers, M. Wilson, F. Garzon, D. Wood, P. Zelenay, K. More, K. Stroh, T. Zawodzinski, J. Boncella, J. E. McGrath, M. Inaba, K. Miyatake, M. Hori, K. Ota, Z. Ogumi, S. Miyata, A. Nishikata, Z. Siroma, Y. Uchimoto, K. Yasuda, K. Kimijima, N. Iwashita, *Chem. Rev.* **2007**, *107*, 3904.
[2] F. A. de Bruijn, V. A. T. Dam, G. J. M. Janssen, *Fuel Cells* **2008**, *08*, 3.
[3] J. F. Wu, X. Z. Yuan, J. J. Martin, H. J. Wang, J. J. Zhang, J. Shen, S. H. Wu, W. Merida, **2008**, *184*, 104.
[4] C. Zhou, M. A. Guerra, Z. M. Qiu, T. A. Zawodzinski, D. A. Schiraldi, *Macromolecules* **2007**, *40*, 8695.
[5] V. O. Mittal, H. R. Kunz, J. M. Fenton, *J. Electrochem. Soc.* **2006**, *153*, A1755.
[6] V. O. Mittal, H. R. Kunz, J. M. Fenton, *J. Electrochem. Soc.* **2007**, *154*, B652.
[7] L. Zhang, S. Mukerjee, *J. Electrochem. Soc.* **2006**, *153*, A1062.
[8] D. Zhao, B. L. Yi, H. M. Zhang, M. L. Liu, *J. Power Sources* **2010**, *195*, 4606.
[9] D. E. Curtin, R. D. Lousenberg, T. J. Henry, P. C. Tangeman, M. E. Tisack, *J. Power Sources* **2004**, *131*, 41.
[10] M. Danilczuk, S. Schlick, F. D. Coms, *Macromolecules* **2009**, *42*, 8943.
[11] D. Zhao, B. L. Yia, H. M. Zhang, H. M. Yu, L. Wang, Y. W. Ma, D. M. Xing, *J. Power Sources* **2009**, *190*, 301.
[12] N. Asano, M. Aoki, S. Suzuki, K. Miyatake, H. Uchida, M. Watababe, *J. Am. Chem. Soc.* **2006**, *128*, 1762.
[13] M. Aoki, N. Asano, K. Miyatake, H. Uchida, M. Watanabe, *J. Electrochem. Soc.* **2006**, *153*, A1154.
[14] S. H. Xiao, H. M. Zhang, C. Bi, Y. N Zhang, Y. M. Ma, X. F. Li, H. X. Zhong, Y. Zhang, *J. Power Sources* **2010**, *195*, 8000.
[15] D. Zhao, B. L. Yi, H. M. Zhang, H. M. Yu, *J. Membr. Sci.* **2010**, *346*, 143.
[16] L. Wang, B. L. Yi, H. M. Zhang, Y. H. Liu, D. M. Xing, Z. G. Shao, Y. H. Cai, *J. Power Sources* **2007**, *167*, 47.
[17] K. A. Sung, W.-K. Kim, K.-H. Oh, M. -J. Choo, K.-W. Nam, J.-K. Park, *J. Power Sources* **2011**, 196, 2483.
[18] H. Dai, H. M. Zhang, H. X. Zhong, X. F. Li, S. H. Xiao, Z. S. Mai, *Int. J. Hydrogen Energy* **2010**, *35*, 4209.
[19] J. Zhu, H. L. Tang, M. Pan, *J. Membr. Sci.* **2008**, *312*, 41.
[20] S. Hommura, K. Kawahara, T. Shimohira, Y. Teraoka, *J. Electrochem. Soc.* **2009**, *155*, A29.
[21] L. Franck-Lacaze, C. Bonnet, E. Choi, J. Moss, S. Pontvianne, H. Poirot, R. Datta, F. Lapicque, *Int. J. Hydrogen Energy*, **2010**, *35*, 10472.
[22] M. A. Hickner, H. Ghassemi, Y. S. Kim, B. R. Einsla, J. E. McGrath, *Chem. Rev.* **2004**, *104*, 4587.
[23] Z. W. Bai, M. F. Durstock, T. D. Dang, *J. Membr. Sci.* **2006**, *281*, 508.
[24] Z. W. Bai, D. Dang, *Macromol. Rapid Commun*. **2006**, *27*, 1271.
[25] K. B. Wiles, F. Wang, J. E. McGrath, *J. Polym. Sci. Part A: Poly.Chem.* **2005**, *43*, 2964.
[26] Z. W. Bai, M. D. Houtz, P. A. Mirau, T. D. Dang, *Polymer* **2007**, *48*, 6598.
[27] L. Q. Shen, G. Y. Xiao, D. Y. Yan, G. M. Sun, *e-Polymers* **2005**, no.031, http://www.e-polymers.org.
[28] H. Dai, H. M. Zhang, Q. T. Luo, Y. Zhang, C. Bi, *J. Power Sources* **2008**, *185*, 19.
[29] J. K. Lee, J. Kerres, *J. Membr. Sci*. **2007**, *294*, 75.
[30] M. Schuster, C. C. de Araujo, V. Atanasov, H. T. Andersen, K. D. Kreuer, J. Maier, *Macromolecules* **2009**, *42*, 3129.
[31] C. Zhang, X. X. Guo, J. H. Fang, H. J. Xu, M. Q. Yuan, B. W. Chen, *J. Power Sources* **2008**, *170*, 42.
[32] W. Li, A. Manthirama, M. D. Guiver, *J. Membr. Sci.* **2010**, *362*, 289.
[33] Y. H. Xue, R. Q. Fu, C. M. Wu, J. Y. Lee, T. W. Xu, *J. Membr. Sci.* **2010**, *350*, 148.
[34] F. Zhang, N. W. Li, Z. M. Cui, S. B. Zhang, S. H. Li, *J. Membr. Sci.* **2008**, *314*, 24.
[35] S.-H Hsiao, M. -H. He, *J. Polym. Sci. Part A: Poly.Chem.* **2001**, *39*, 4014.
[36] J. H. Li, H. Y. Yu, *J. Polym. Sci. Part A: Poly.Chem.* **2007**, *45*, 2273.
[37] H. S. Lee, A. Roy, O. Lane, M. Lee, J. E. McGrath, *J. Polym. Sci. Part A: Poly. Chem.* **2010**, *48*, 214.
[38] A. S. Badami, O. Lane, H. S. Lee, A. Roy, J. E. McGrath, *J. Membr. Sci.* **2009**, *333*, 1.
[39] Z. Zhou, S. W. Li, Y. L. Zhang, M. L. Liu, W. Li, *J. Am. Chem. Soc.* **2005**, *127*, 10824
[40] N. Tan, G. Y. Xiao, D. Y. Yan, *Polym. Bull.* **2009**, *62*, 593.
[41] D. Xing, J. Kerres, *Polym. Adv. Technol.* **2006**, *17*, 591.
[42] J. Kamada, K. Koynov, C. Corten, A. Juhari, J. A. Yoon, M. W. Urban, A. C. Balazs, K. Matyjaszewski, *Macromolecules* **2010**, *43*, 4133.
[43] K.-S Lee, M.-H. Jeong, J.-P. Lee, J. -S. Lee, *Macromolecules* **2009**, *42*, 584.
[44] N. Tan, G. Y. Xiao, D. Y. Yan, *Chem. Mater.* **2010**, *22*, 1022.
[45] L. Y. Gui, C. J. Zhang, S. Kang, N. Tan, G. Y. Xiao, D. Y. Yan, *Int. J. Hydrogen Energy* **2010**, *35*, 2436.
[46] M. Schuster, C. C. de Araujo, V. Atanasov, H. T. Andersen, K. D. Kreuer, J. Maier, *Macromolecules* **2009**, *42*, 3129.
[47] L. Wang, D. Zhao, H. M. Zhang, D. M. Xing, B. L. Yi, *Electrochem. Solid-State Lett.* **2008**, *11*, B201.